Processing of Allied Air Forces World War II Strategic Air Reconnaissance Imagery

RUWEI NIE[1], MICHAEL CRAMER[1] & PATRICK LUBIG[2]

***Abstract**: Historical Aerial Images (HAIs) can provide long time series record of landscape change and landcover dynamic monitoring. With the development of computer vision, the challenges of interpretation and analysis of HAIs can be solved using methods like Structure from Motion (SfM). The key step of the application is to georeference the imagery to the reference coordinates system with a set of Ground Control Points (GCP). A coarse-to-fine approach was proposed to determine the position of GCPs and to generate georeferenced orthoimage and Digital Surface Model (DSM) in the study area. The georeferencing error was assessed by means of Root Mean Square Error (RMSE) computation. In total 4 steps of adding GCPs in weak areas with large RMSE values were implemented, to improve the georeferencing accuracy with a minimal number of GCPs expressed in terms of nGCPs/km^2. The refined accuracy for X, Y and Z axis were 1.63 m, 2.49 m and 7.59 m, respectively, with a ratio of 1.80 GCPs/km^2.*

1 Introduction

1.1 Motivation

In the years from 1939 to 1945, a transformational growth in aerial reconnaissance happened, especially in Britain and then in the United States. An amount of millions of historical aerial images was obtained by aerial reconnaissance in the time from 1938 until the end of the war and even beyond (MEIXNER & ECKSTEIN 2016). These Historical Aerial Images (HAIs) covered an aera of the majority of today's European countries and are now available in the allied archives such as the National Collection of Aerial Photography (NCAP) or the National Archives and Records Administration Washington (NARA). Recently, with the digitization of archival film-based historical aerial reconnaissance imagery, there is now free access through spatial data infrastructures and web services in many countries (GIORDANO et al. 2017). With the access of HAIs, a lot of research and imagery analysis were conducted by experts for the land survey and bomb detection. For example, the Luftbilddatenbank Dr. Carls GmbH did an extensive research and acquisition of stereoscopic interpretable series of aerial photographs from the time between 1938 and 1955 (MEIXNER & ECKSTEIN 2016). The Landesamt für Geoinformation und Landentwicklung in Baden-Württemberg has a collection of HAIs from the pre- and post-war period to produce true orthophotos and 3D models for landcover analysis and research. Like other historical records, the collection and interpretation of aerial reconnaissance intelligence are now a crucial contribution to ecosystem mapping and landscape features representation in small scale (TUOMINEN & PEKKARINEN 2005). Besides, they also provide long time series record of landscape

[1] Universität Stuttgart, Institut für Photogrammetrie (ifp), Geschwister-Scholl-Str. 24D, 70174 Stuttgart, E-Mail: michelle_11_15@outlook.com, michael.cramer@ifp.uni-stuttgart.de
[2] LBA Luftbildauswertung GmbH, Ludwigstraße 17B, 70176 Stuttgart, E-Mail: patrick.lubig@lba-luftbildauswertung.de

 DOI: 10.24407/KXP:1796029637

change and temporally continuous and spatially complete landcover dynamic monitoring (PAINE & KISER 2003).

However, along with the contributes and advantages of HAIs there are very specific characteristics of the imagery: analog photographs are acquired with different cameras in different acquisition conditions, the image quality is of huge variation and the images exhibit highly heterogeneous spatial resolutions (GIORDANO et al. 2018); the digital images are often scanned from old analog photographs, there remains only a coarse image localization. Metadata such as the physical size of the analog photos, the focal length of the camera and the camera calibration reports are not always available (MICHELETTI et al. 2015). Fortunately, with the rapid development of computer vision and the automatic feature-matching algorithms, Structure from Motion (SfM) resolves the problem of recovering the 3D structure from a series of overlapping aerial images. The approach uses conventional photogrammetric processing combined with computer vision SfM techniques to produce a robust solution that can self-calibrate and overcome the challenges of unknown uncalibrated cameras, inaccurate GPS systems and environmental conditions (EISENBEIß 2009). Hence, this method provides a possibility to the usage of the HAIs which are lack of ground control information and precise camera parameters to reconstruct the former geometry of landscape surfaces (NAGARAIAN & SCHENK 2016).

The paper is based on the research of a master thesis project in corporation of the Institut für Photogrammetrie (ifp) and LBA Luftbildauswertung GmbH. The practical application of the work in LBA requires to georeference the HAIs from World War II to present-day reference orthoimages or reference maps in order to search for the remains of arial bombing activities and to analyze the possibility of the unexploded ordnance on the land or underneath the earth surface. Hence, it is extremely important to locate the accurate position of the bombing area which is shown in the HAIs related to the present-day reference maps. As a result of this, the horizontal accuracy of the georeferencing process is of great interest for the practical work and is the most essential part for the applications. As known from the presented research, the georeferencing of HAIs is very difficult to implement and the accuracy can be very different because of the variance of the quality of the images and the condition of the study areas. One commonly applied method is to select Ground Control Points (GCPs) as ground reference manually by visual comparison between the scanned HAIs and the present-day orthoimages or Digital Surface Model (DSM) in GIS environment. Researches were conducted using this method: ONIGA et al. (2020) selected 150 GCPs in a 0.08 km^2 area and obtained a mean accuracy of 2.10 m with 1875 GCP/km^2; PERSIA et al. (2020) applied 75 GCPs in 67 HAIs covering 550 km^2 area surface and the mean accuracy was 2.66 m with 0.14 GCP/km^2. The goal of the master project was to obtain satisfying horizontal accuracy of georeferencing the HAIs at a lower cost of manual work as for a minimal number of GCPs, and to search for possible methods to improve the vertical accuracy at most. In the study area, the desired threshold for horizontal error was set to be below 5 m, while the expected vertical error was set to be below 10 m.

1.2 System Workflow

The system was designed subsequently according to the goals and requirements of the project. A coarse to fine approach was provided to generate fine absolute oriented orthoimage product. In the

coarse to fine approach, the first step was to compute a coarse absolute image orientation without the ground reference. The second step was to use coarse oriented orthoimage comparing with the present-day reference orthoimages and DSM to determine the GCPs, then with the ground reference the coarse absolute orientation was georeferenced to the reference coordinate system as fine absolute oriented orthoimage. The major challenge was the determination of ground references information, hence the georeferencing step was extremely essential to the accuracy of final absolute orientation. For the georeferencing process, a two-step method was proposed to achieve the desired accuracy with optimal GCPs. The Check Points (ChPs) provided a possibility to check and evaluate the georeferencing quality. At the end of the coarse to fine approach, the value of the ChPs coordinates error was assessed by the index Root Mean Square Error (RMSE). If the index RMSE was beyond the desired threshold of horizontal and vertical accuracy, the number of GCPs would then be increased to rerun the process until the desired accuracy is obtained.

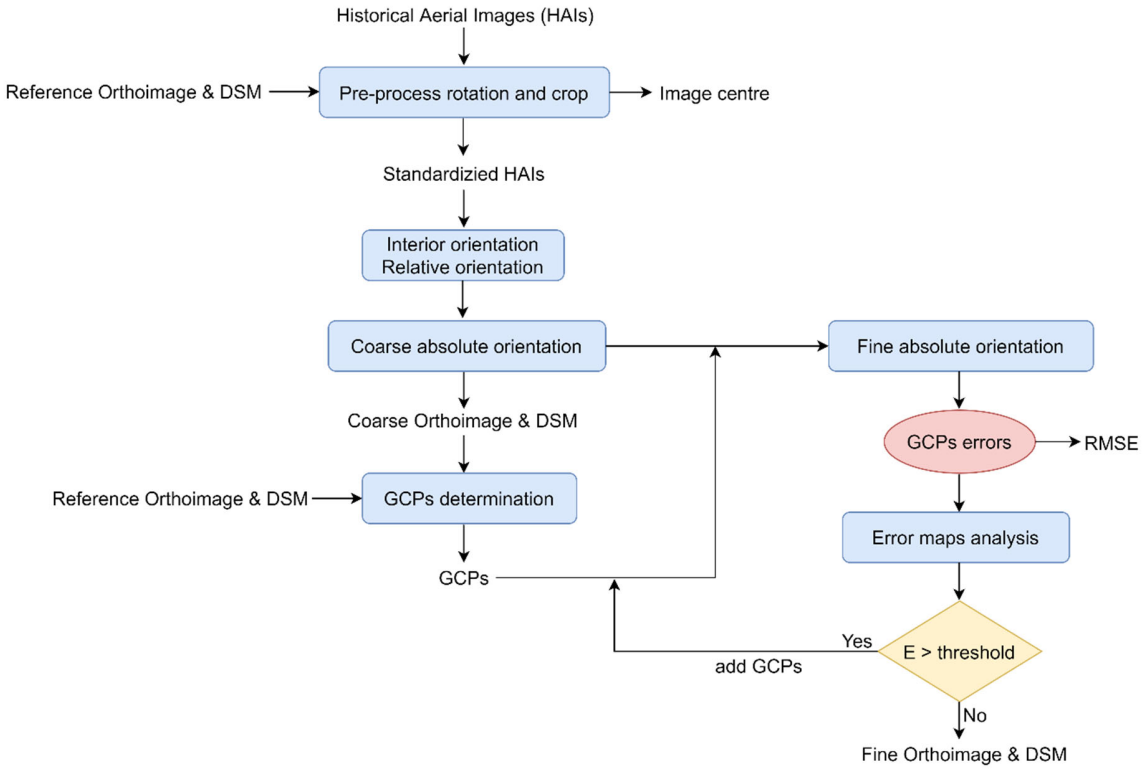

Fig. 1: System workflow

The designed workflow illustrated in Fig. 1 includes three main parts: the image pre-processing, the data processing, and the result analysis. In the image pre-processing part, the original HAIs were standardized in MATLAB, and the image centers were obtained. In the data processing part, the proposed coarse to fine approach was conducted with the GCPs determination in Agisoft Metashape. In the result analysis part, the GCPs coordinates error and the ChPs coordinates error were assessed to be RMSE and the error values were analyzed and visualized in error map productions in QGIS. The number of GCPs would be increased and added in the areas with high error values indicated by the error map to improve the georeferencing accuracy.

2 Data Sources and Study Area

2.1 Study Area

The study area as shown in Fig. 2 on the left side is in the capital city Erfurt in state Thüringen of Germany. In total 21 overlapping aerial images were processed covering a surface of approximately 20 km^2. The area was selected because the data sources were free available from Thüringen-Geoportal Open Geodata. What is more important is that the medieval town center of the city Erfurt with its many cultural monuments was not severely devastated by area bombings in the second World War, which made it easier to locate the ground reference for georeferencing. Reconstructing the aerial sightseeing from above with the HAIs from the end of the war and comparing the reconstructed scene with the reference orthoimages provided a method to discover the land cover change and city rebuilding after the second World War. Besides, the determination of the position of the area bombings is essential for the safety and stability of human activities and construction development. A second more rural study area with different landcover and identical features was applied to verify the general effectivity of the proposed approach but will not be discussed in detail (NIE 2021).

A sample of 21 black and white aerial images from two flight missions token above the city Erfurt were acquired as the source aerial images. As shown in Fig. 2 on the right side, the flight project 194539 contains 6 overlapping aerial images (green) which were captured on 23.03.1945; the flight project 194574 contains 15 overlapping aerial images (red) which were captured on 08.04.1945. Both flight projects were back and forth in the approximate direction of east-west. The 21 images were divided into three image groups, where there was not enough overlapping area in-between.

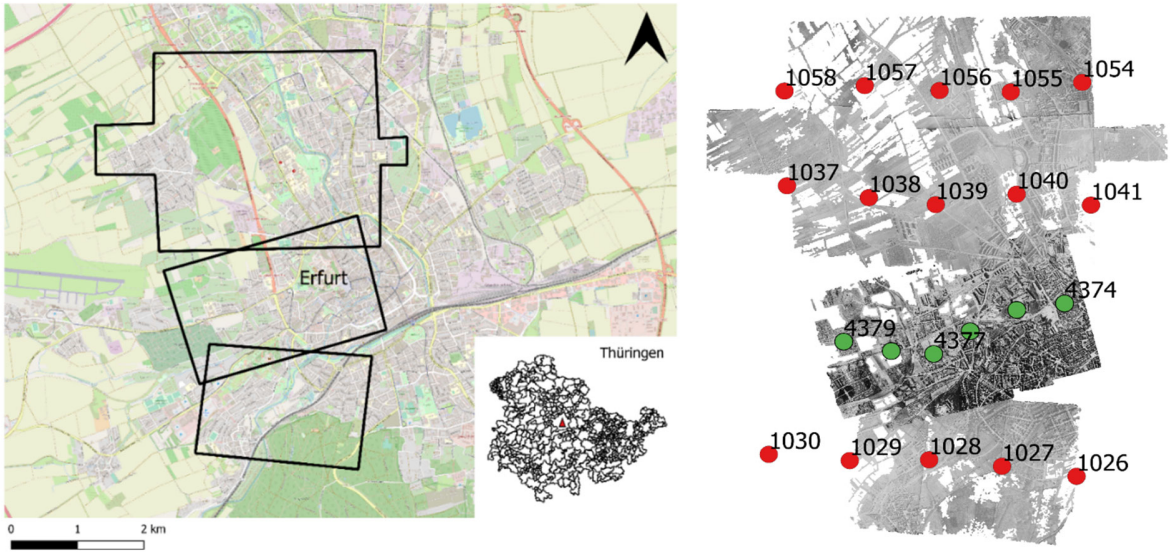

Fig. 2: Study area in Erfurt (left) and perspective center positions of two flight missions (right)

2.2 The Historical Aerial Images

Shown in Fig. 3 on the left side are two examples of the aerial images from flight missions 194539 and 194574. The zoom-in detailed identical features of the same scene from two different flight missions are shown on the right side. It is noteworthy that the two images are of different physical

size and image brightness. The image quality is not optimal to identify the features of streets and building structures. Additionally, the digital aerial images were scanned from analog aerial images and provided in GeoTIFF format. Hence, there was no calibration report for the camera information available, the manufacture information and interior orientation parameters were missing as well.

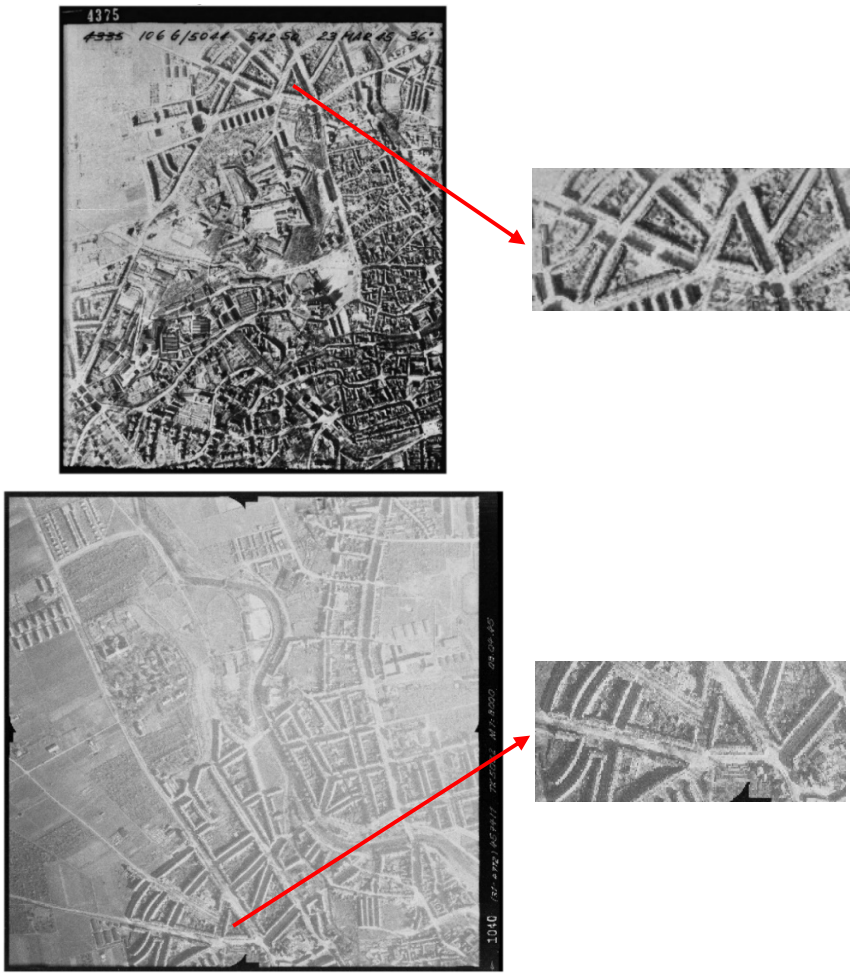

Fig. 3: Historical aerial images (left) with identical features (right) (top: 194539, bottom: 194574)

2.3 The Reference Orthoimage and DSM

The reference orthoimage and DSM shown in Fig. 4 were acquired from Thüringen-Geoportal Open Geodata in ETRS89 / UTM 32N coordinates system. The reference orthoimage colored in RGB were acquired on 23.03.2020 with a ground sampling distance of 0.2 m and standard deviation of 0.4 m. The State Office for Surveying and Geoinformation of Thüringen regularly used the airborne laser scanning to produce digital terrain and surface models, the DSM used as reference height model was obtained in January 2014 with a ground sampling distance of 1 m. The reference orthoimages and DSM rasters with the size of 1 km * 1 km were merged into one orthoimage and reference DSM covering the whole study area. The terrain in the north-east area is lower than in the south-west area, and the height difference is relatively large up to 170 m.

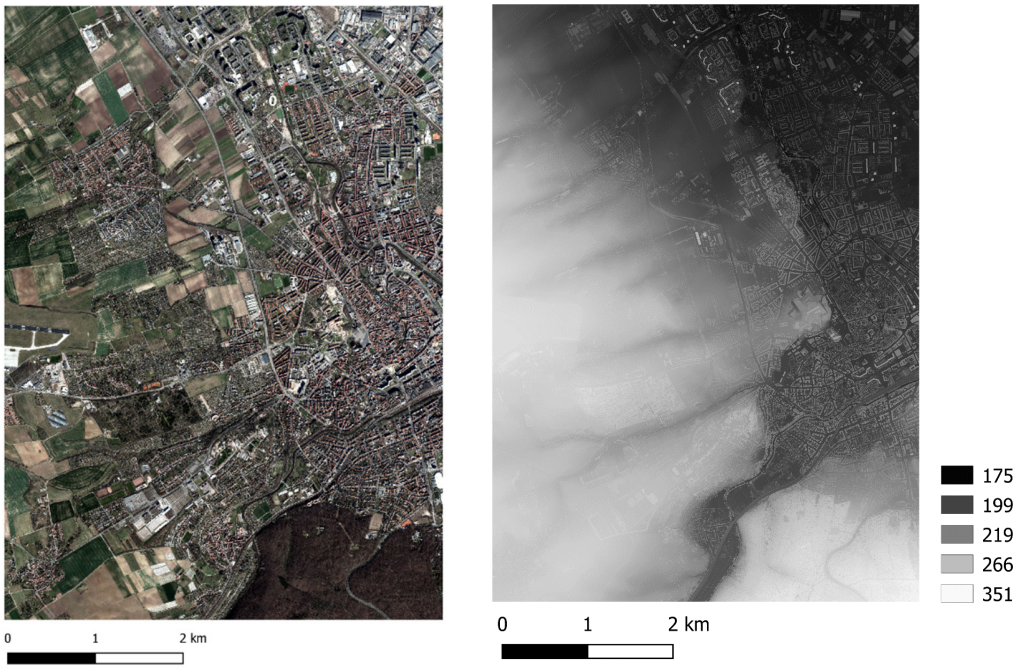

Fig. 4: Reference orthoimage (left) and DSM (right)

2.4 Ground Control Points

The GCPs are important to scale and orient the final orthoimage to the reference coordinates system and to assess the georeferencing accuracy of the ChPs. The horizontal and vertical positions of the selected control points were uncertain because they were identified manually using the present-day reference orthoimage and reference DSM. The land cover and the terrain surface might have changed significantly after a long time of manual constructions and human activities. To determine the uncertainty of the control points positions is extremely difficult. In order to minimize the uncertainty of the spatial positions of the control points, the selection of the positions where the GCPs and ChPs locate is essential. In this project, the control points were selected as the identities which were assumed to be stable and considered unchanged over time. The example features of GCPs and ChPs selection are shown in Fig. 5.

The study area is covering a large area of the city center and a small part of forests and farming fields. In the urban area, the GCPs and ChPs were mainly selected on the roof edges and some manmade features. For these identical features, the horizontal coordinates which were computed from reference orthoimage are more accurate than the vertical coordinates which were computed from reference DSM. A small change in the selected horizontal position on the roof edges might lead to a big difference in vertical height. Hence, they are usually used as 2D horizontal GCPs. The intersections of roads were used as reference points as well and are usually accurate in vertical and used as vertical GCPs. In the farming fields, the intersections of farming quarter were considered to be stable features. The stable features were selected as GCPs and ChPs manually by visual comparison of the coarse orthoimages of the three image groups and the reference orthoimage in QGIS. The X and Y coordinates were computed from the reference orthoimage

while the Z coordinates were extrapolated from the reference DSM. The reference coordinates system of the reference points was established in ETRS89 / UTM 32N.

Fig. 5: Reference points selection features (left: HAIs, right: reference orthoimage)

3 Implementation and Processing

In order to bring the scale and orientation of the coarse orthoimages to the reference coordinates system, the GCPs and ChPs were introduced to the georeferencing process. As shown in Fig. 6, in total 4 steps of adding GCPs to search for an optimal number of GCPs to improve the georeferencing results were implemented. The GCPs and ChPs were selected on the surfaces assumed to be stable over time and were distributed in the whole study area. In step 1, 12 GCPs in black triangles were selected in the corner of the image groups. More GCPs shown in red triangles, green triangles and blue triangles were added in each step, which were in total 18 GCPs in step 2, 27 GCPs in step 3 and 36 GCPs in step 4. The total surface of the study area is approximately 20 km^2. Hence, the index nGCP/km^2 in each step was 0.60 GCP/km^2, 0.90 GCP/km^2, 1.35 GCP/km^2 and 1.80 GCP/km^2. The number and position of the 24 ChPs remained unchanged, which provided check and evaluation to the georeferencing quality. The GCPs and ChPs in each step were added to the process in Agisoft Metashape and tagged to the HAIs manually. Besides, the georeferenced orthoimage and DSM of each step were generated as final georeferenced products.

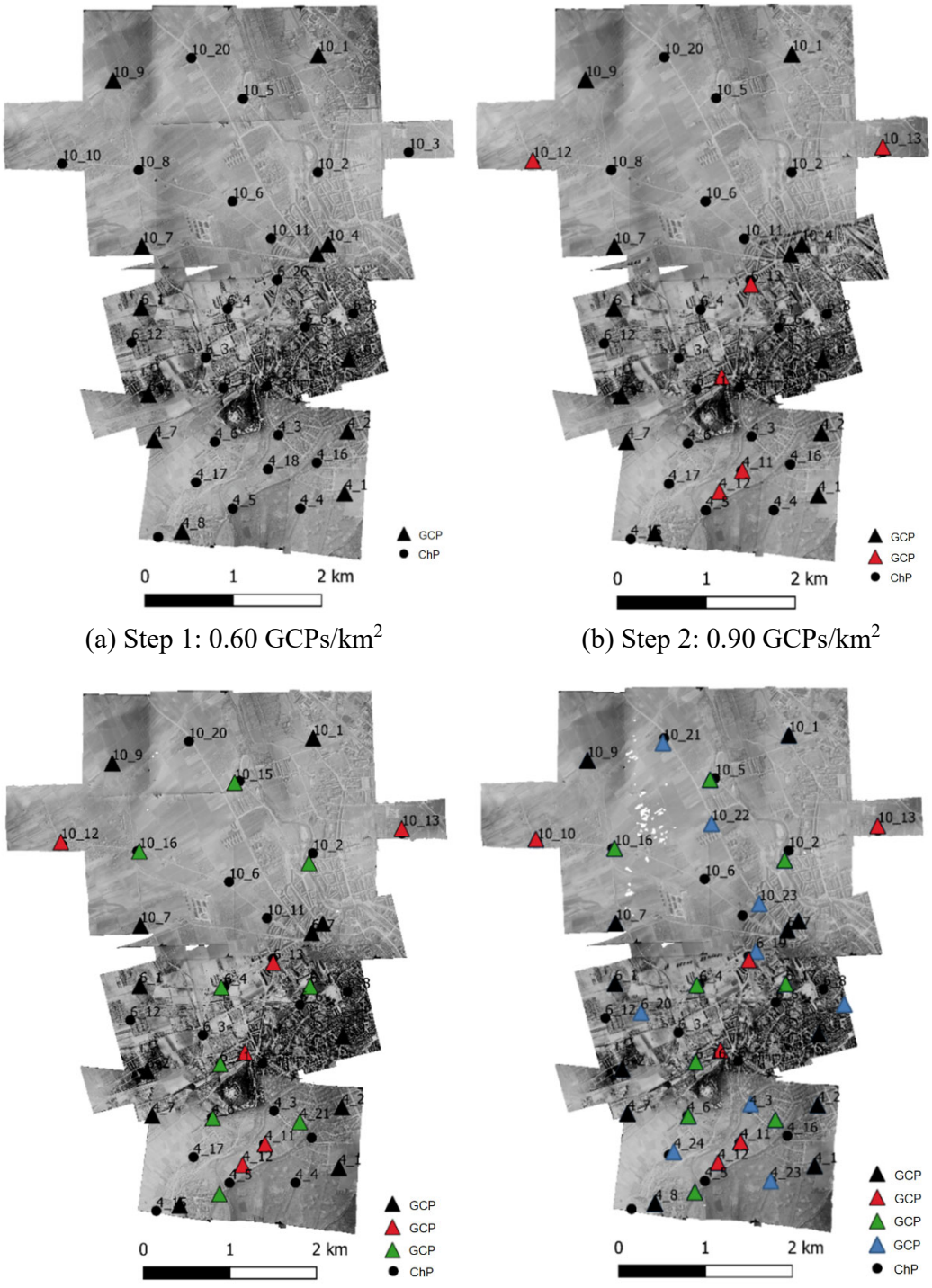

(a) Step 1: 0.60 GCPs/km^2 (b) Step 2: 0.90 GCPs/km^2

(c) Step 3: 1.35 GCPs/km^2 (d) Step 4: 1.80 GCPs/km^2

Fig. 6: GCPs and ChPs in 4 steps

4 Results Analysis

4.1 RMSE of GCPs and ChPs

Once the aerial images were aligned with the selected GCPs and ChPs, the RMSE values referring to the corresponding GCPs and the ChPs in each step were calculated and exported, the labels of each selected GCPs and ChPS were listed along with the X, Y, Z coordinates, with X axis pointing towards east and Y axis pointing towards north. The error values of each GCPs and ChPs along the X, Y, Z axes were listed as X error, Y error and Z error, respectively (Tab. 1).

Tab. 1: RMSE (m) values referring to the corresponding GCPs and the ChPs in each step

Steps	Num.	X error	Y error	Z error	XY error	total error
Step 1	12 GCPs	2.12	2.29	0.52	3.12	3.16
	24 ChPs	4.23	5.45	42.27	6.90	42.83
Step 2	18 GCPs	2.36	2.25	0.38	3.26	3.28
	24 ChPs	2.74	4.18	28.04	4.99	28.48
Step 3	27 GCPs	1.86	1.98	0.83	2.72	2.84
	24 ChPs	2.83	3.57	12.53	4.56	13.33
Step 4	36 GCPs	1.99	1.86	0.67	2.73	2.81
	24 ChPs	2.05	3.48	18.65	4.04	19.08
Refine Step	36 GCPs	1.95	1.86	0.67	2.69	2.77
	24 ChPs	1.63	2.49	7.59	2.98	8.15

The RMSE values referring to all the 24 ChPs along X, Y, Z axes in each step are illustrated in Fig. 7. The horizontal axis consists of the 4 steps of adding GCPs for georeferencing and refine step with new ChPs selections. The left vertical axis in blue is the scale for X and Y errors, while the right vertical axis in red is the scale for Z errors. X error, Y error and Z error are represented in square, triangle and circle, the values of the errors along three directions in each step are marked clearly as well.

Pay attention to the RMSE values comparison of the ChPs, it is clear that from step 1 to step 2, the errors along the X and Y directions are decreasing slightly while the error along the Z direction is decreasing dramatically from 42.27 m to 28.04 m. The horizontal accuracy is satisfied in step 2 but the vertical error still overcomes the desired vertical accuracy. Hence more GCPs were added in step 3 to reduce the vertical error. From step 2 to step 3, the X error is slightly increasing while the Y error is slightly decreasing, which might be explained by the flight line direction. As mentioned, the flight direction was east-west direction which is along the X axis of easting. The Y axis is perpendicular to the X axis pointing northing. The Z error continues to reduce from 28.04 m to 12.53 m, which is not acceptable for vertical accuracy. In order to verify the prediction that the vertical error continues decreasing when more GCPs were added, step 4 was applied and proved that the Z error did not continue decreasing as predicted but increased from 12.53 m to 18.65 m. It means that there is no necessity to invest more manual work of selecting GCPs for

georeferencing for more steps. Hence the system design stopped in step 4 and the vertical accuracy in step 3 is considered the best georeferencing results we might obtain by adding GCPs.
In step 3, the X error and Y error are 2.83 m and 3.57 m, which are absolutely acceptable for horizontal accuracy considering the study area is 20 km^2 and only 27 GCPs were applied. The Z error with 12.53 m is, however, relatively large for vertical accuracy. The possible reasons might be the GCPs selection procedure. Since adding GCPs in step 4 did not improve the Z accuracy, other investments were applied to improve the accuracy in vertical direction in refine step (see section 4.3).

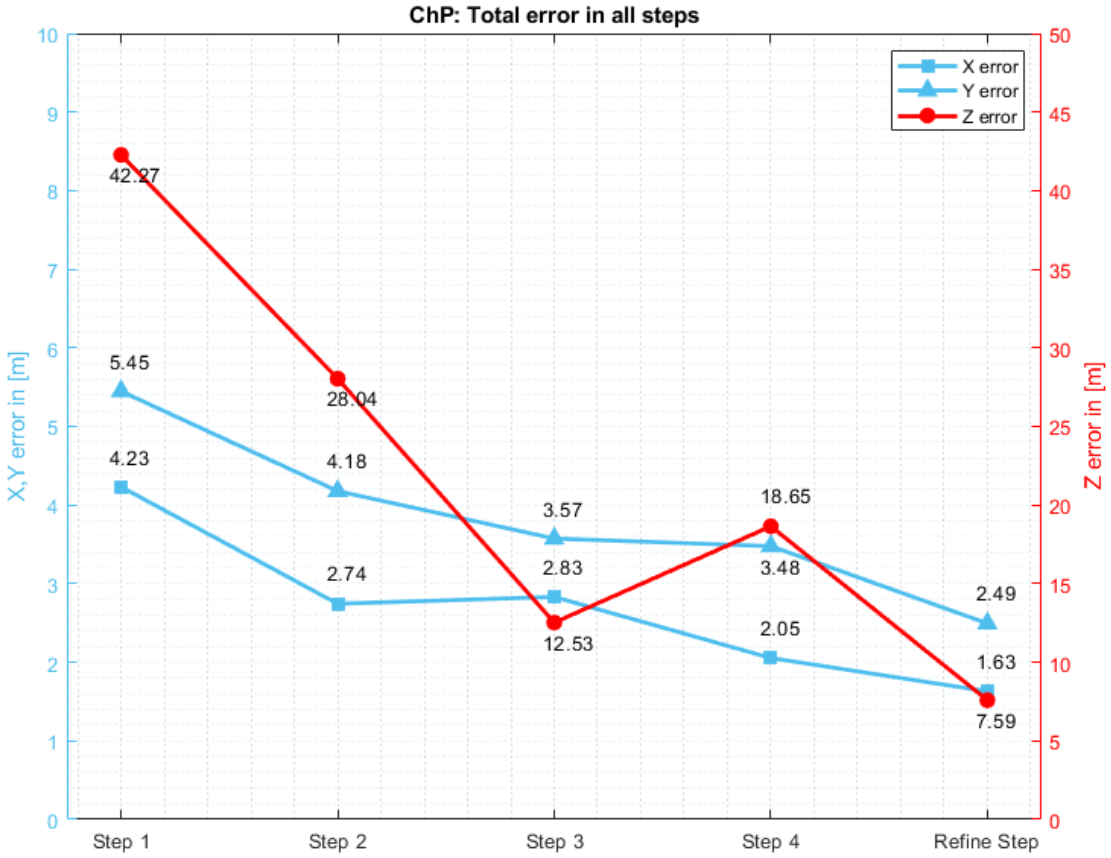

Fig. 7: RMSE values comparison of ChPs in all steps

4.2 Error Maps

To understand the spatial distributions of the RMSE values of the GCPs and the ChPs, the error maps of the GCP errors and ChP errors along X, Y, Z axes in step 3 are illustrated in Fig. 8. Error maps of the GCPs and ChPs along X axis, Y axis and Z axis are shown in red, green and blue with the triangles representing the GCPs errors and the circle points representing the ChPs errors. The color of each point represents the value of the errors. The value of the error changes from minimum to maximum as the color of the points changes from light to dark: the darker the point, the larger the error value. More GCPs were added in the areas with large absolute ChPs error values which were shown in the error maps in each step to improve the georeferencing accuracy.

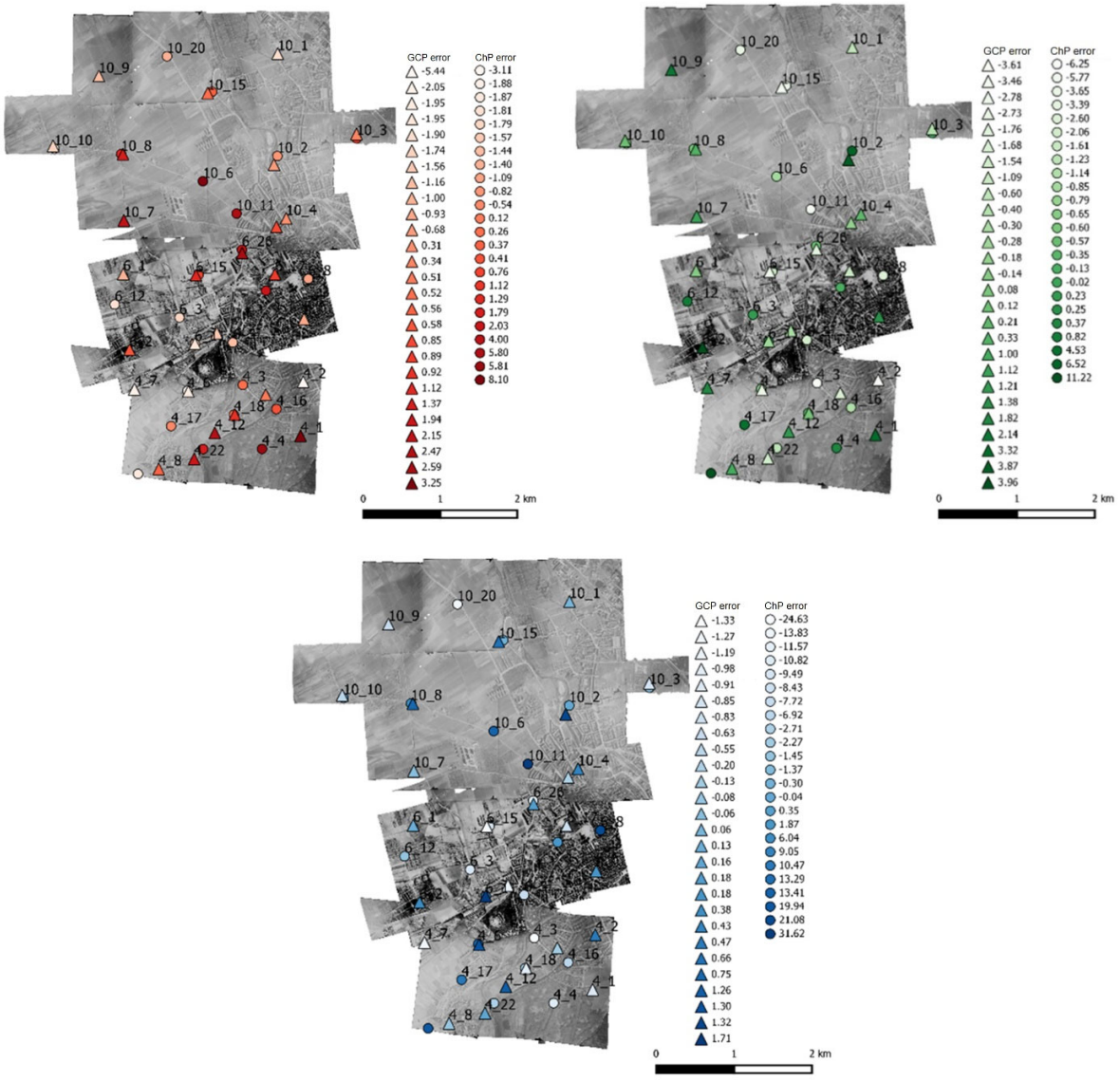

Fig. 8: Error maps along X (red), Y (green), Z (blue) axis in step 3

4.3 Refine Results

The study area in the city Erfurt was mainly covered by buildings and a small part of forests and farming fields. Hence, the horizontal error values were small and could be improved by adding GCPs easily because it was not difficult to find the identical features to determine the GCPs and the positions of the GCPs were relatively accurate. On the contrary, the vertical error values were the most uncertain element and could not be improved by adding GCPs in step 4. The possible error source might be that the GCPs and ChPs were selected mostly on the identical features such as the roof edges (Fig. 9). It might be the fact that the points were located on the road with height of 194 m besides the roof with height of 213 m or on the tree leaves above the roof, which could make a difference of 10 m to 15 m in vertical.

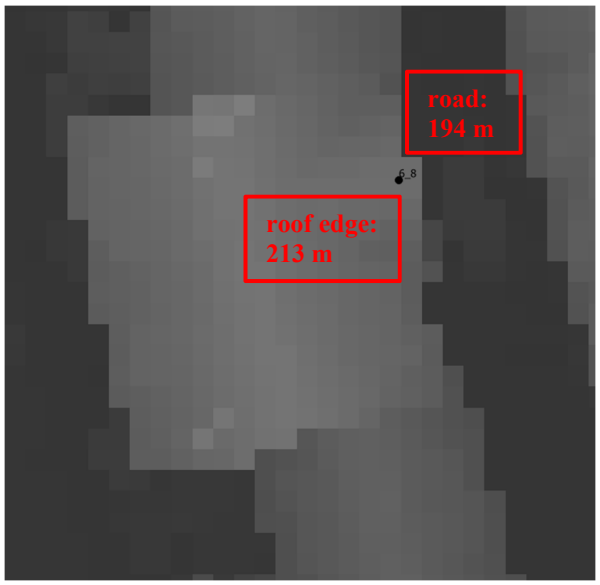

Fig. 9: Error source of ChPs selection

The vertical accuracy of the georeferencing process is of most uncertainty and adding GCPs in the areas with large errors could not improve the vertical accuracy in both study areas after 3 steps. Other methods were applied to determine the possible influence on vertical georeferencing elements, such as adding manual tie points to the matching images, separating the location GCPs and height GCPs. Unfortunately, all these methods did not work on improving the vertical accuracy. The method of the project was to increase the number of GCPs but did not change the position and quantity of the ChPs in the 4 steps. However, as explained before, the GCPs and ChPs determination procedure might have influenced the vertical accuracy and caused a difference of 10 m to 15 m in vertical direction. Hence, the ChPs with large RMSE values in Z axis were considered as outliers and were deleted in order to refine the vertical accuracy. After deleting the outliers, new ChPs were selected as shown in Fig. 10. The ChP 6_8 at the roof edge was with a high Z error and was deleted as an outlier and a new ChP 6_8 was selected in a new position.
Based on the error map along Z axis in step 4, in total 4 ChPs with large Z error values were newly selected. The RMSE values referring to the 36 GCPs and 24 ChPs with new selections are shown as refine step in Tab. 1 and from Fig. 7 we can see that the Z error reduced from 18.65 m in step 4 to 7.59 m in refine step. Additionally, it is noteworthy that the horizontal error values decreased as well with the new selections of ChPs. From the result that both the horizontal accuracy and vertical accuracy increased and the minimum and the maximum Z error values reduced dramatically, there is indeed a problem with GCPs and ChPs selection procedures, which caused the error values in Z axis. Hence, the advice for future works is to select the points correctly in the position where there is no great height difference between the selected point and the surroundings. Besides, the result indicates that the accuracy might be continuously improved when the ChPs with large error values are new selected.

Fig. 10: ChPs outlier (left) and new selection (right)

5 Conclusion and Future Work

The goal was to georeference the HAIs at a lower cost of manual work as for a minimal number of GCPs to obtain the desired horizontal accuracy, and to search for the possible methods to improve the vertical accuracy. The project has provided a workflow to process the images in a coarse to fine approach, in which the aerial images were processed without any camera calibration information as for coarse processed orthoimages, and then the coarse orthoimages were georeferenced with the selected GCPs and the ChPs to produce the error maps of X, Y, Z error values, according to which more GCPs were selected and added in the areas affected by large errors to achieve a higher accuracy for horizontal and vertical. Finally, when the accuracy could not be improved by adding more GCPs in the weak areas with large errors, the final fine georeferenced orthoimages were generated and mapped.

Two study areas with different landcover and identical features were tested with the workflow proposed in the project. In the study area in Erfurt, the best accuracy obtained by adding GCPs were 2.83 m for X axis, 3.57 m for Y axis, 12.53 m for Z axis, respectively, with a minimum quantity of only 27 GCPs in the area of 20 km^2. In the more rural study area, the best accuracy obtained by adding GCPs were 11.23 m for X axis, 6.47 m for Y axis, 12.80 m for Z axis, respectively. The horizontal error values were large compared with the horizontal error values of the study area in Erfurt but considered to be acceptable with a minimal number of only 12 GCPs in an area of 16.6 km^2.

In both study areas, the vertical accuracy stopped to improve after 3 steps of adding more GCPs in the weak areas. This fact proves that it is not the case that the more GCPs the better accuracy but there is an optimal number of GCPs with a lower cost of manual work within a certain area. The index nGCPs/km^2 which means the GCPs rate per unit area, is an effective index to improve the efficiency of georeferencing process: in the urban area with obvious identical features such as building roof and streets intersection, the ratio is 1.35 GCPs/km^2; in the area with vegetation landcover and farming field, the ratio is 0.72 GCPs/km^2. The index nGCPs/km^2 is now utilized as

a reference for practical application of the work in LBA, to reduce the manual investigation to select GCPs in different landcover and surface conditions and to georeference the HAIs with a desired horizontal accuracy better than 5 m.
Additionally, the vertical accuracy in both study areas was approximately 12 m in step 3. The selection procedure of GCPs and ChPs caused a difference of 10 m to 15 m in vertical direction, which could not be improved by adding GCPs to georeferencing process. After new selection of ChPs in refine step, the vertical accuracy was improved to be 7.59 m. The research of refining the vertical accuracy indicated how important the determination procedure of GCPs and ChPs was. Therefore, a method of how and where to locate the position of GCPs for the practical application was suggested: to select identical features which are not direct near trees or other vegetations and are not at the exact corner of the roof edges near streets or roads.
Many practical applications require accurate horizontal georeferencing of old images and present-day maps referring to the present regions. From the final result analysis, it is apparent that the selection of the GCPs and ChPs is the fundamental procedure in the georeferencing process of HAIs. The final refined accuracy of the proposed methodology satisfied the expectation: the RMSE values for X, Y and Z axis were 1.63 m, 2.49 m and 7.59 m, respectively, with a ratio of 1.80 GCPs/km^2. The workflow provides a method to georeference the HAIs efficiently with the index nGCPs/km^2 and automatically with the computer vision SfM techniques.
However, it is worth mentioning that the method of adding GCPs in weak areas with large errors was not investigated in this work. The GCPs were added in or within the areas where the RMSE values were large but without a certain rule and the distribution of the GCPs was not regulated as well. Theoretically, to define the optimal number of GCPs in a certain size of study area statistically is of significant research potential. In addition, to determine how the spatial distribution of the GCPs as well as the ChPs affects the final georeferencing accuracy is also an interesting topic to follow on. Another topic which might deserve further research lies in different study areas with different conditions, such as areas with great land cover change, which could make it difficult to find GCPs, or areas with large terrain change, which makes it even more challenging to determine error values in the vertical direction.

6 References

EISENBEIß, H., 2009: UAV photogrammetry. Doctoral dissertation, ETH Zurich, https://doi.org/10.3929/ethz-a-005939264.

GIORDANO, S., LE BRIS, A. & MALLET, C., 2017: Fully automatic analysis of archival aerial images current status and challenges. IEEE Joint Urban Remote Sensing Event (JURSE), 1-4, https://doi.org/10.1109/JURSE.2017.7924620.

GIORDANO, S., LE BRIS, A. & MALLET, C., 2018: Toward automatic georeferencing of archival aerial photogrammetric surveys. ISPRS Annals of Photogrammetry, Remote Sensing and Spatial Information Sciences, **4**, 105-112. https://hal.archives-ouvertes.fr/hal-02386709.

MICHELETTI, N., LANE, S. N. & CHANDLER, J. H., 2015: Application of archival aerial photogrammetry to quantify climate forcing of alpine landscapes. The Photogrammetric Record, **30**(150), 143-165. https://doi.org/10.1111/phor.12099.

MEIXNER, P. & ECKSTEIN, M., 2016: MULTI-TEMPORAL ANALYSIS OF WWII RECONNAISSANCE PHOTOS. International Archives of the Photogrammetry, Remote Sensing & Spatial Information Sciences, **41**. https://doi.org/10.5194/isprs-archives-XLI-B8-973-2016.

NAGARAJAN, S. & SCHENK, T., 2016: Feature-based registration of historical aerial images by Area Minimization. ISPRS Journal of Photogrammetry and Remote Sensing, **116**, 15-23. https://doi.org/10.1016/j.isprsjprs.2016.02.012.

NIE, R., 2021: Processing of Allied Air Forces World War II Strategic Air Reconnaissance Imagery. Master dissertation, Universität Stuttgart, Institut für Photogrammetrie, https://www.ifp.uni-stuttgart.de/lehre/masterarbeiten/625-Nie.

ONIGA, V. E., BREABAN, A. I., PFEIFER, N. & CHIRILA, C., 2020: Determining the suitable number of ground control points for UAS images georeferencing by varying number and spatial distribution. Remote Sensing, **12**(5), 876. https://doi.org/10.3390/rs12050876.

PAINE, D. P. & KISER, J. D., 2012: Aerial photography and image interpretation. John Wiley & Sons.

PERSIA, M., BARCA, E., GRECO, R., MARZULLI, M. I. & TARTARINO, P., 2020: Archival aerial images georeferencing: a geostatistically-based approach for improving orthophoto accuracy with minimal number of ground control points. Remote Sensing, **12**(14), 2232. https://doi.org/10.3390/rs12142232.

TUOMINEN, S. & PEKKARINEN, A., 2005: Performance of different spectral and textural aerial photograph features in multi-source forest inventory. Remote sensing of Environment, **94**(2), 256-268. https://doi.org/10.1016/j.rse.2004.10.001.